Journal of Solid State Chemistry 240 (2016) 43–48

Contents lists available at ScienceDirect

Journal of Solid State Chemistry

journal homepage: www.elsevier.com/locate/jssc

Direct optical band gap measurement in polycrystalline semiconductors: A critical look at the Tauc method

Alex Dolgonos [a], Thomas O. Mason [a], Kenneth R. Poeppelmeier [b,*]

[a] Department of Materials Science and Engineering, Northwestern University, Evanston, IL 60208, USA
[b] Department of Chemistry, Northwestern University, Evanston, IL 60208, USA

ARTICLE INFO

Article history:
Received 19 January 2016
Received in revised form
9 May 2016
Accepted 10 May 2016
Available online 11 May 2016

Keywords:
Band gap
Diffuse-reflectance
Photoluminescence
ITO
Degenerate doping

ABSTRACT

The direct optical band gap of semiconductors is traditionally measured by extrapolating the linear region of the square of the absorption curve to the *x*-axis, and a variation of this method, developed by Tauc, has also been widely used. The application of the Tauc method to crystalline materials is rooted in misconception–and traditional linear extrapolation methods are inappropriate for use on degenerate semiconductors, where the occupation of conduction band energy states cannot be ignored. A new method is proposed for extracting a direct optical band gap from absorption spectra of degenerately-doped bulk semiconductors. This method was applied to pseudo-absorption spectra of Sn-doped In_2O_3 (ITO)—converted from diffuse-reflectance measurements on bulk specimens. The results of this analysis were corroborated by room-temperature photoluminescence excitation measurements, which yielded values of optical band gap and Burstein–Moss shift that are consistent with previous studies on In_2O_3 single crystals and thin films.

1. Introduction

Accurate determination of a material's optical band gap (E_g) is critical in predicting applicability and performance in optoelectronic devices. The most widely utilized techniques for E_g measurement involve absorption-based spectroscopic techniques, such as transmission measurements on thin films [1–4] or diffuse-reflectance (DR) measurements on bulk specimens [5,6]. Such techniques are preferable for bulk property measurement because they avoid the confounding of bulk properties by surface effects, owing to the large penetration depths of photons in the energy range of the band gaps of most semiconductors. Higher-energy photoelectron spectroscopy measurements, on the other hand, are limited by the relatively short photoelectron inelastic mean free paths, which are on the order of a few nanometers [7–9].

In determining the optical band gap of a degenerately-doped semiconductor, several band-altering effects must be taken into account. Fundamental band gap renormalization (ΔE_g^{RN}) results in a narrowing of the fundamental band gap, owing to doping-induced electron-electron and electron-impurity scattering [10], whereas the Burstein-Moss shift (ΔE_g^{BM}) has an opposing effect on E_g [11]. The combination of these factors necessitates distinguishing nomenclature when referring to the fundamental band gap of an undoped semiconductor (E_{g0}), the renormalized fundamental band gap of a doped semiconductor ($W = E_{g0} + \Delta E_g^{RN}$), and the optical band gap ($E_g = E_{g0} + \Delta E_g^{RN} + \Delta E_g^{BM} = W + \Delta E_g^{BM}$).

1.1. Traditional methods

The generally accepted practice in the experimental determination of E_g from bulk specimens is to first convert DR spectra to pseudo-absorption spectra $F(R)$ via the Kubelka–Munk transformation [12]:

$$F(R) = \frac{K}{S} = \frac{(1-R)^2}{2R} \tag{1}$$

where R is the reflectance of an infinitely thick specimen, and K and S are the absorption and scattering coefficients, respectively. The scattering coefficients of most materials are relatively invariant along the visible range of the optical spectrum, so S can be treated as a constant; thus, $F(R)$ can be treated as a pseudo-absorption function.

$F(R)$ is then substituted for α in

$$\alpha = A(h\nu - W)^{\gamma}, \tag{2}$$

where γ equals $\frac{1}{2}$ or 2 for a material with a direct or indirect band gap, respectively [13]. In the case of indirect transitions, the relation is slightly complicated by phonon absorption and emission

* Corresponding author.
E-mail address: krp@northwestern.edu (K.R. Poeppelmeier).

http://dx.doi.org/10.1016/j.jssc.2016.05.010
0022-4596/

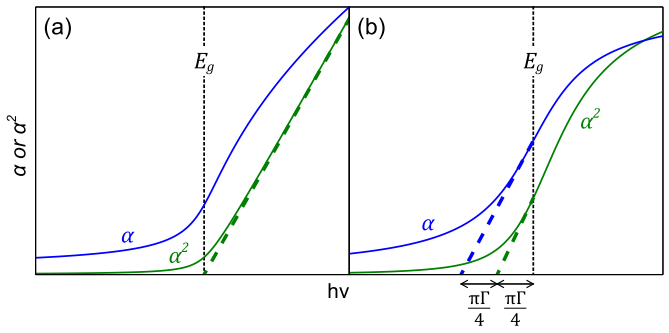

Fig. 1. (a) The traditional method of obtaining E_g from the extrapolated x-intercept from the linear region of the α^2 vs. $h\nu$ curve, as is applicable for non-degenerate semiconductors. In (b), as derived in the text, the difference between the two extrapolated x-intercepts (from both the α and α^2 curves) is added to the one from the α^2 vs. $h\nu$ curve to obtain the proper value of E_g for a degenerate semiconductor.

processes. The right side of Eq. (2) must therefore be scaled by the probability of these processes–which are obtained through Bose-Einstein statistics–but a similar linear relation persists. E_g is then found as the extrapolated x-intercept of the linear region of the plot of $[F(R)]^{1/\gamma}$ vs. $h\nu$, as shown in Fig. 1(a).

Another widely-used practice is to utilize the Tauc equation [14–16], which is essentially equivalent to Eq. (2), but with α being replaced by $\alpha h\nu$ [17–19]. However, the use of the Tauc method to calculate the band gap in crystalline/polycrystalline materials is subject to scrutiny; the relation derived by Tauc [19] (and separately by Davis and Mott [20]) was intended for use with amorphous materials, using the assumption that amorphous materials contain a localization of energy states (an element of disorder is in fact present in polycrystalline materials, though the extent of this disorder is far greater in amorphous semiconductors than in their polycrystalline counterparts). All derivations also assumed that transitions need not conserve momentum–an assumption that would not necessarily hold in a polycrystalline semiconductor with a direct band gap.

Other extrapolation-based methods make use of different proportionalities relating photon energy and the band gap. The Sokolov gap, for example, assumes band linearity–as opposed to the parabolicity assumed by Tauc–resulting in a proportionality identical to that of the Tauc equation, but with a cube root relation. The Cody gap, on the other hand, assumes an unchanging dipole matrix element with photon energy, resulting in a proportionality of $\sqrt{\alpha/h\nu}$ [21]. Additionally, optical gaps of amorphous materials have also been defined by utilizing the photon energy correspong to a pre-specified absorption coefficient (commonly 10^3 or 10^4 cm^{-1}). However, like the Tauc method, these relations were all developed under the assumption of energy state localization.

A more subtle complication in the extraction of an E_g value from absorption spectra involves the convolution of the measurement by the broadening of initial (i) and final (f) states of the generated electron-hole pair from optical absorption (a result of time-dependent perturbation theory) [22], which is accounted for by the broadening time constant τ in

$$R = \frac{2}{\hbar^2}\sum_{i,f}|\langle i|V|f\rangle|^2\frac{\tau^{-1}}{(\omega-\omega_{if})^2+\tau^{-2}}(P_i-P_f), \tag{3}$$

where R is the transition rate between the initial and final states, P is the probability that the state is occupied, and $\omega_{if} = (E_i - E_f)/\hbar$.

E_g calculations based on misconceptions or misinterpretations can lead to inaccurate measurements and therefore misleading conclusions. The objective of this work is to establish a more accurate method in determining E_g from DR (or absorption) measurements in bulk polycrystalline direct band gap semiconductors.

1.2. Proposed methods

Assuming interband transitions between a filled parabolic valence band and a partially-filled parabolic conduction band, Eq. (3) can be re-written as [23]

$$R \propto \int_{x_0}^{\infty}(x+h\nu-W)^{1/2}\frac{\Gamma}{x^2+\Gamma^2}(1-P_c)dx, \tag{4}$$

where

$$x \equiv \frac{\hbar^2k^2}{2m_{vc}^*} + W - h\nu, \tag{5}$$

$$x_0 \equiv \Delta E_g^{BM} + W - h\nu, \tag{6}$$

Γ is an energy broadening term equal to $\hbar/\tau$, P_c is the occupation probability of conduction band states (a Fermi-Dirac distribution), and m_{vc}^* is the reduced effective mass of charge carriers.

If the Fermi level is sufficiently lower than the conduction band minimum, as is the case in a non-degenerate semiconductor, then Eq. (4) can be simplified and solved analytically, assuming $P_c = \Delta E_g^{BM} = 0$ and $x_0 = W - h\nu$:

$$\alpha \propto \left[\sqrt{(h\nu-W)^2+\Gamma^2}-(h\nu-W)\right]^{-1/2}. \tag{7}$$

Squaring Eq. (7) and taking a Laurent series expansion at large values of $h\nu$ yields, to first order,

$$\alpha^2 \propto (h\nu - W). \tag{8}$$

Such a derivation indicates that, in the case of non-degenerate semiconductors, the approach implied from Eq. (2) remained valid. However, to estimate Γ and to better account for baseline intensity, Eq. (7) should be fit to the absorption spectrum.

In the case of a degenerate semiconductor, the approximations used for Eq. (7) cannot be made. However, if a sharply-peaked Lorentzian term in Eq. (4) is assumed (relatively small Γ), then the relation for photon absorption involving transitions to a partially occupied conduction band can be simplified to [23]

$$\alpha \propto 1 - \frac{2}{\pi}\arctan\left(\frac{E_g-h\nu}{\Gamma}\right). \tag{9}$$

A series expansion about E_g then yields (to first order)

$$\alpha \propto 1 - \frac{2}{\pi\Gamma}(E_g - h\nu). \tag{10}$$

Thus, the extrapolated x-intercept of an α vs. $h\nu$ plot corresponds to $E_g - \frac{\pi}{2}\Gamma$.

Contrast this with the linear relationship between α^2 and $h\nu$ that results from direct transitions to an empty band [Eq. (8)], with W found by extrapolating the linear region of this plot to the x-axis (which is true for the limit of $\Gamma \to 0$, i. e. if Fermi's golden rule is assumed). A more accurate linear dependence of α^2 on $h\nu$ can be found by taking a series expansion of α^2—based on the relationship in Eq. (9)—about E_g to first order, obtaining

$$\alpha^2 \propto 1 - \frac{4}{\pi\Gamma}(E_g - h\nu). \tag{11}$$

An extrapolation of the linear region of the α^2 vs. $h\nu$ plot to the x-axis would therefore yield $E_g - \frac{\pi}{4}\Gamma$.

Thus, the two extrapolated x-intercepts can be combined to empirically determine E_g by the process illustrated in Fig. 1(b). This procedure is analogous to the methods described in Section 1.1, with the notable difference being the adjustment for the energy broadening term Γ. As is evident from Fig. 1(b), a standard linear

extrapolation method informed by Eq. (2) would underestimate the optical band gap by $\pi\Gamma/4$. An important note is that, because the linear approximations in Eqs. (10) and (11) apply only around $h\nu = E_g$, the results must be checked for self-consistency. Again, to better account for baseline absorption, a more accurate measurement of E_g can be made by fitting Eq. (9) to the absorption spectrum. In this case, E_g would correspond to the photon energy at the inflection point of the α vs. $h\nu$ curve. This is also the result derived by Gibbs et al. for narrow band gap thermoelectric materials via computation of the Fermi distribution around the absorption edge [5].

To demonstrate the viability of the above methodology in determining its E_g, Sn-doped In_2O_3 (ITO) was used as the experimental test case–chosen for its widespread applicability in optoelectronic devices [3,24,25] as well as for its wide band gap and amenability to degenerate doping [26–28]. Additionally, the optical absorption characteristics of In_2O_3 can be modeled by direct allowed interband transitions, rendering Eq. (3) applicable to the material. The nature of optical transitions in In_2O_3 has been subject of some contention [29–32]; however, it can be reconciled through evidence in previous studies. Absorption measurements on single-crystal In_2O_3 have shown a weak dependence of α on temperature [31], suggesting optical transitions are not phonon-assisted. Though direct optical transitions in In_2O_3 have been shown to be dipole-forbidden at the Γ point [32], calculations on similar direct band gap oxides have demonstrated a significant increase in direct transition probability as the k-vector is shifted off-center [33]. The Burstein-Moss shift–which involves the filling of the lowest-energy conduction band states at the Γ point–further necessitates that the final energy states in optical excitations be offset from Γ [1]. These factors suggests that the dipole-allowed off-center direct transitions are the most probable in ITO, and are therefore responsible for the optical behavior in the material.

2. Experimental

2.1. Solid-state synthesis

Bulk ceramic samples (~2 g) were synthesized from initial oxide powders of In_2O_3 (99.994%; Alfa Aesar, Ward Hill, MA) and SnO_2 (99.99%; Sigma Aldrich) by the procedure described in detail in Ref. [28]. The In_2O_3 specimen was sintered at 1250 °C for 24 h and subsequently annealed at 750 °C for 4 h—to avoid auto-reduction at elevated temperature—before being cooled to room temperature at 5 °C/min. The ITO specimen, which was maximally-doped with 2 mol% SnO_2 [28], was sintered at 1350 °C for 72 h before being quenched in air to maximize the electron concentration. Phase purity was confirmed by X-ray diffraction using a Rigaku DMAX diffractometer (Rigaku Corporation, Tokyo, Japan).

To ensure degeneracy of the ITO specimen, room-temperature conductivity (σ) measurements were performed on both the ITO and the reference In_2O_3 samples by methods described in detail by Hong et al. [34]. Geometry corrections to the conductivity were performed as outlined by Smits et al. for a pellet in four-probe configuration [35], and porosity corrections were calculated by the Bruggeman symmetric model [36], where pores were assumed to be an insulating secondary phase. The conductivities of the two materials were found to be 4380 and 10 S/cm for ITO and In_2O_3, respectively, confirming the doping nature of the specimens.

2.2. Diffuse-reflectance

DR was measured using a Lambda 1050 UV/Vis/NIR spectrophotometer with an integrating sphere attachment (Perkin-Elmer, Oak Brook, IL). Spectra were taken from 250 to 800 nm with baselines of 0% R and 100% R taken using pressed polytetrafluoroethylene powder compacts. The DR spectra were converted by the Kubelka-Munk transformation to generate pseudo-absorption spectra. These were then analyzed by the linear extrapolation methods illustrated in Fig. 1—as well as by fitting Eqs. (7) (to the In_2O_3 data) or (9) (to the ITO data) to obtain E_g values, where the absorption behavior is modeled by allowed direct transitions.

2.3. Photoluminescence

To corroborate the DR measurements, photoluminescence excitation (PLE) measurements of the bulk ITO specimen were taken at room temperature. Relaxation from E_g to W results in peak PL emission at the W energy after excitation by an incident photon energy corresponding to the E_g energy [39,40]. Furthermore, since excitons can be assumed to be unbound at room temperature, excitonic effects on emission can be disregarded [41]. Using a Horiba Fluorolog 3 (Horiba Scientific, Edison, NJ), the wavelength of the excitation beam was ranged from 310 to 394 nm by 2 nm intervals, and emission spectra were collected from 400 to 520 nm in 0.265 nm intervals. To reduce the effect of noise on the PLE data, second-order Savitzky-Golay smoothing [42] was used to determine the emission and excitation values corresponding to the maximum emission intensity.

3. Results and discussion

The DR measurements (Fig. 2) reveal a fundamental band gap of 2.95(1) eV in undoped In_2O_3, which is in close agreement with photoelectron spectroscopy studies on single crystals that indicate a band gap of 2.93 eV [43]. An E_g of 3.38(1) was obtained by fitting Eq. (9) to the pseudo-absorption spectrum in ITO. This value is notably lower than the values of ~4 eV obtained from absorption studies of ITO thin films [2,4]. This discrepancy can be attributed to the difference between the two sample types. Because direct optical transitions are dipole-forbidden at the Γ point, the absorption in thin films is dominated by excitations from valence band levels that are at least 0.8 eV below the VBM [32], resulting in an E_g above 4 eV. Conversely, the effect of off-Γ absorption, which occurs in both thin films and bulk, is larger in bulk specimens, owing to their longer optical path length. Shifting the k-vector off the zone center has been shown to dramatically increase the probability of dipole-allowed transitions [33], thereby allowing optical excitations to occur from the VBM.

The agreement between the new linear extrapolation method [Fig. 2(e)] and the curve-fitting method [Fig. 2(f)] in determining the E_g of the material supports the viability of the former method in estimating the band gap from absorption spectra. Using the traditional method [Eq. (2)] would result in an underestimation of E_g by approximately 0.2 eV. This error can be seen from the linear extrapolation of the $[F(R)]^2$ curve in Fig. 2(e).

The PLE emission intensity peak at 3.35(1) eV in degenerately doped bulk ITO (Fig. 3) supports the DR-derived E_g value, differing by only ~0.03 eV. The extracted W value–when analyzed against the W measurement from the In_2O_3 DR data–indicates a reasonable band gap renormalization of about -0.14 eV, and the difference in the excitation and emission energies at the peak intensity corresponds to a ΔE_g^{BM} of 0.54(2) eV. According to the relationships calculated by Hamberg et al. [23] and Walsh et al. [44] relating the carrier concentration in ITO and its associated ΔE_g^{BM}, the electron concentration in this sample is in the range of $2 - 3 \times 10^{20}$ cm^{-3}. A reasonable carrier mobility in the range of 30–40 cm^2 V^{-1} s^{-1}

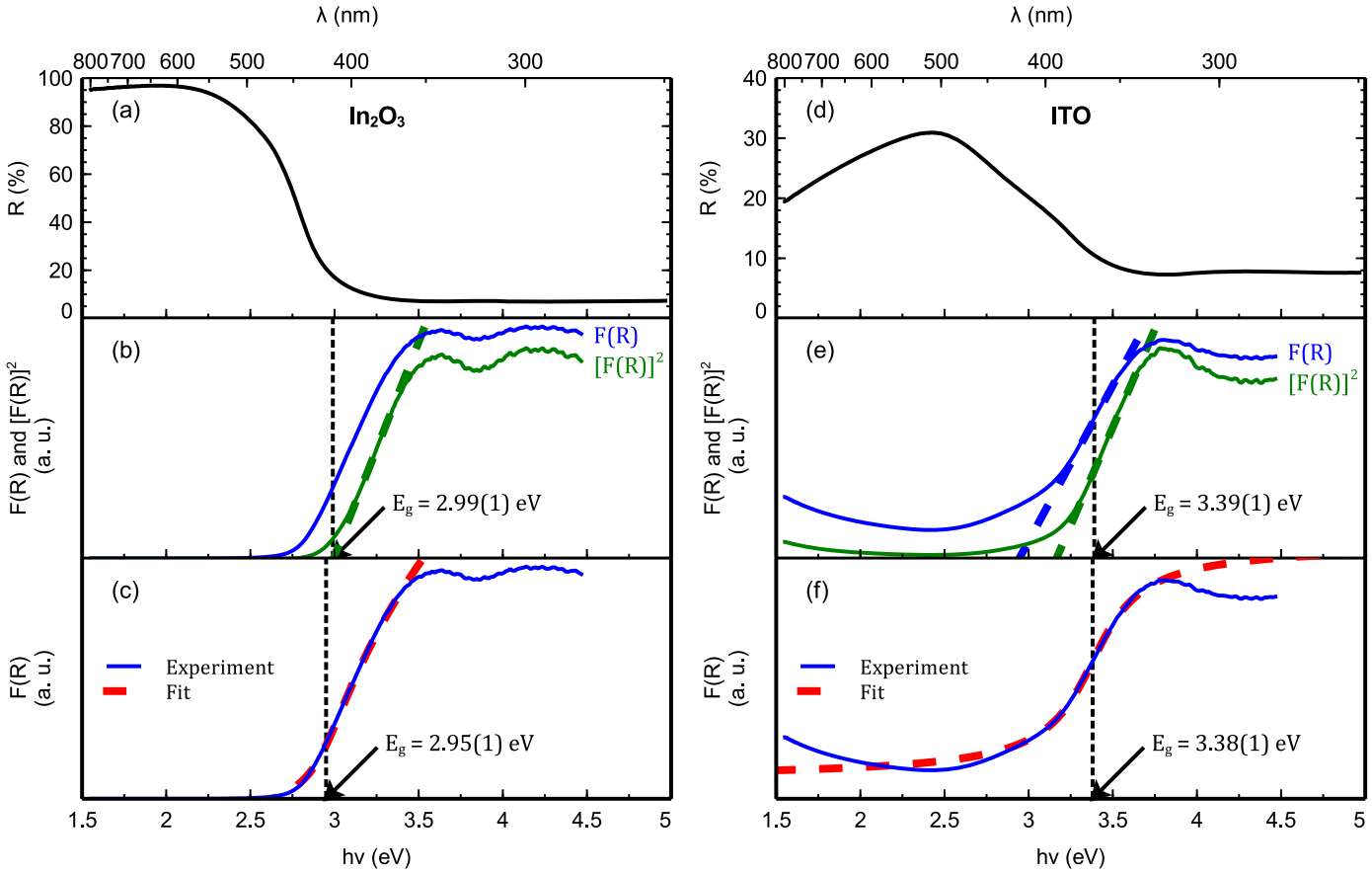

Fig. 2. From top to bottom: DR spectra of (a) undoped In_2O_3 and (d) degenerately-doped ITO, respectively; E_g determination by the linear extrapolation method illustrated in Fig. 1 for (b) In_2O_3 and (e) ITO; and E_g determination (c) by fitting Eq. (7) to the pseudo-absorption spectrum of In_2O_3, and (f) by fitting Eq. (9) to that of ITO.

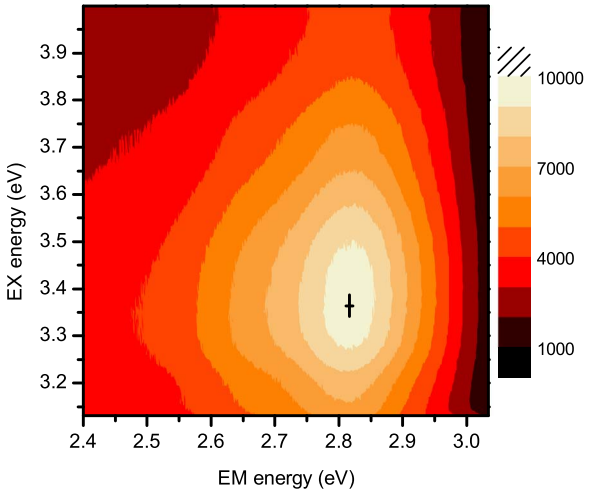

Fig. 3. Representative PLE measurement of bulk ITO, where the black lines correspond to the uncertainties in the position of the intensity peak. The peak emission energy corresponds to a W of 2.81(1) eV, and the excitation energy at the intensity peak indicates an E_g of 3.35(1) eV.

[45,46] would imply an electron concentration within the same order of magnitude.

4. Conclusions

Conventional techniques of extracting E_g from absorption spectra of direct-gap crystalline semiconductors were shown to be inappropriate in the case of degenerately-doped bulk materials. The Tauc method is applicable only to materials in which a localization of energy states can be assumed–such as in amorphous materials and nanoparticles–and applying Eq. (8) to a degenerately-doped material results in an underestimation of E_g. Based on the calculations of Hamberg and Granqvist [1], the extent of this underestimation ($\frac{\pi}{4}\Gamma$) can be found by taking the difference in the extrapolated x-intercepts of the linear portions of the α vs. $h\nu$ and α^2 vs. $h\nu$ graphs.

The technique proposed in this work was applied in determining the E_g of bulk ITO from DR spectra. The E_g value derived in this manner was corroborated by PLE measurements, which were also used to reveal the renormalized fundamental band gap (W) of the material. The polycrystalline nature of the bulk ITO specimens used for this work–as well as the ΔE_g^{BM} that results from their degenerate doping–allow optical transitions to occur offset from the Brillouin zone center, thereby making dipole-allowed direct transitions the dominant optical absorption mechanism. To confirm the validity of these assumptions, it is recommended that calculations similar to those conducted on SnO_2 [33] be made on In_2O_3 in determining the optical dipole-matrix elements off the zone center.

The combined DR and PLE measurements yielded values of band gap and Burstein-Moss shift that are consistent with previous absorption and photoelectron spectroscopy studies on In_2O_3 single crystals [31,43] and thin films [32]. Furthermore, the difference between the E_g of ~3.3 eV reported in this work for bulk polycrystalline ITO and the widely-reported values of ~4 eV in ITO thin films [2,4] confirms the work of Walsh et al. [32] in calculating optical transitions from the top 0.8 eV states in the valence band of In_2O_3 to be dipole-forbidden at the Γ point.

Acknowledgments

This research was supported by the U. S. Department of Energy, Office of Basic Energy Sciences, Division of Materials Sciences and Engineering under Award No. DE-FG02–08ER46536 and by the Air Products Foundation through the Air Products and Chemicals, Inc. Graduate Fellowship. The authors would like to acknowledge the generous assistance of Heather Arnold in the Department of Materials Science and Engineering at Northwestern University in acquiring photoluminescence spectra. Discussions with Dr. Andreas Klein in the Surface Science Division of the Institute of Materials Science at the Darmstadt University of Technology have also been invaluable in the understanding the energy structure of indium oxide and in the interpretation of optical spectra. Diffuse-reflectance spectra were obtained at the Keck Biophysics Facility at Northwestern University, which is supported by grants from the W. M. Keck Foundation, Northwestern University, the NIH, the Rice Foundation, and the Robert H. Lurie Comprehensive Cancer Center. X-ray diffraction and photoluminescence measurements were performed at Northwestern University utilizing instruments in, respectively, the J. B. Cohen X-ray Diffraction Facility and the Energy Materials Laboratory within the Department of Materials Science and Engineering; both facilities are supported by the MRSEC program of the National Science Foundation (NSF-DMR-1121262).

Appendix A. Supplementary data

Supplementary data associated with this article can be found in the online version at http://dx.doi.org/10.1016/j.jssc.2016.05.010.

References

[1] I. Hamberg, C.G. Granqvist, Evaporated Sn-doped In_2O_3 films basic optical properties and applications to energy-efficient windows, J. Appl. Phys. 60 (11) (1986) R123–R159, http://dx.doi.org/10.1063/1.337534 ⟨⟩.
[2] F.M. Amanullah, K.J. Pratap, V. Hari Babu, Characterization of isochronally and isothermally annealed indium tin oxide thin films, Thin Solid Films 254 (1–2) (1995) 28–32, http://dx.doi.org/10.1016/0254–0584(93)90201-V.
[3] C.G. Granqvist, A. Hultåker, Transparent and conducting ITO films new developments and applications, Thin Solid Films 411 (1) (2002) 1–5, http://dx.doi.org/10.1016/S0040–6090(02)00163–3.
[4] N.M. Torkaman, Y. Ganjkhanlou, M. Kazemzad, H.H. Dabaghi, M. Keyanpour-Rad, Crystallographic parameters and electro-optical constants in ITO thin films, Mater. Charact. 61 (3) (2010) 362–370, http://dx.doi.org/10.1016/j.matchar.2009.12.020 ⟨⟩.
[5] Z.M. Gibbs, A. Lalonde, G.J. Snyder, Optical band gap and the Burstein-Moss effect in iodine doped PbTe using diffuse reflectance infrared Fourier transform spectroscopy, New J. Phys. 15 (1) (2013) 075020, http://dx.doi.org/10.1088/1367–2630/15/7/075020.
[6] A. Dolgonos, K. Lam, K.R. Poeppelmeier, A.J. Freeman, T.O. Mason, Electronic and optical properties of $Ga_{3-x}In_{5+x}Sn_2O_{16}$: an experimental and theoretical study, J. Appl. Phys. 115 (1) (2014) 013703, http://dx.doi.org/10.1063/1.4861130 ⟨⟩.
[7] S.P. Harvey, T.O. Mason, C. Körber, Y. Gassenbauer, A. Klein, Evidence for surface dipole modifications in In_2O_3-based transparent conductors, Appl. Phys. Lett. 92 (25) (2008) 252106, http://dx.doi.org/10.1063/1.2953435 ⟨⟩.
[8] S.P. Harvey, T.O. Mason, C. Körber, A. Klein, Bulk defect chemistry and surface electronic behavior of Zn, Sn codoped In_2O_3 transparent conducting oxides, Phys. Chem. Chem. Phys. 11 (17) (2009) 3099–3104, http://dx.doi.org/10.1039/b905911n ⟨⟩.
[9] A. Klein, C. Körber, A. Wachau, F. Säuberlich, Y. Gassenbauer, R. Schafranek, S. P. Harvey, T.O. Mason, Surface potentials of magnetron sputtered transparent conducting oxides, Thin Solid Films 518 (4) (2009) 1197–1203, http://dx.doi.org/10.1016/j.tsf.2009.05.057, URL ⟨⟩.
[10] K.-F. Berggren, B.E. Sernelius, Band-gap narrowing in heavily doped many-valley semiconductors, Phys. Rev. B 24 (4) (1981) 1971–1986.
[11] E. Burstein, Anomalous optical absorption limit in InSb, Phys. Rev. Lett. 93 (2) (1954) 632–633.
[12] P. Kubelka, F. Munk, An article on optics of paint layers, Z. Tech. Phys. 12 (1931) 593–603.
[13] J.I. Pankove, Fundamental Absorption, in: Optical Processes in Semiconductors, Courier Dover Publications, New York, NY, 1971, Ch. Absorption, pp. 34–52.
[14] Y. Natsume, H. Sakata, Zinc oxide films prepared by sol-gel spin-coating, Thin Solid Films 372 (1–2) (2000) 30–36.
[15] G.G. Valle, P. Hammer, S.H. Pulcinelli, C.V. Santilli, Transparent and conductive ZnO:Al thin films prepared by sol-gel dip-coating, J. Eur. Ceram. Soc. 24 (6) (2004) 1009–1013, http://dx.doi.org/10.1016/S0955–2219(03)00597–1, URL ⟨⟩.
[16] G.K. Paul, S. Bandyopadhyay, S.K. Sen, S. Sen, Structural, optical and electrical studies on sol-gel deposited Zr doped ZnO films, Mater. Chem. Phys. 79 (1) (2003) 71–75.
[17] J. Tauc, R. Grigorovici, A. Vancu, Optical properties and electronic structure of amorphous germanium, Phys. Status Solidi 15 (2) (1966) 627–637.
[18] J. Tauc, Optical properties and electronic structure of amorphous Ge and Si, Mater. Res. Bull. 3 (1) (1968) 37–46.
[19] J. Tauc, High Absorption Region, in: J. Tauc (Ed.), Amorphous and Liquid Semiconductors, Springer US, London and New York, 1974, pp. 173–178 (Ch. Optical Pr).
[20] E.A. Davis, N.F. Mott, Conduction in non-crystalline systems V. Conductivity, optical absorption and photoconductivity in amorphous semiconductors, Philos. Mag. 22 (179) (1970) 903–922.
[21] G.D. Cody, T. Tiedje, B. Abeles, B. Brooks, Y. Goldstein, Disorder and the optical-absorption edge of hydrogenated amorphous silicon, Phys. Rev. Lett. 47 (20) (1981) 1480–1483, http://dx.doi.org/10.1103/PhysRevLett.47.1480.
[22] G.H. Wannier, Quantum relaxation theory of collisions; line broadening, in: Elements of Solid State Theory, Cambridge University Press, Cambridge, England, 1959, Ch. Ohm's Law, pp. 212–217.
[23] I. Hamberg, C.G. Granqvist, K.-F. Berggren, B.E. Sernelius, L. Engström, Band-gap widening in heavily Sn-doped In_2O_3, Phys. Rev. B 30 (6) (1984) 3240–3249.
[24] D.S. Ginley, C. Bright, Transparent conducting oxides, MRS Bull. 25 (8) (2000) 15–18, http://dx.doi.org/10.1557/mrs2000.256.
[25] C.G. Granqvist, Transparent conductors as solar energy materials: a panoramic review, Sol. Energy Mat. Sol. C 91 (17) (2007) 1529–1598, http://dx.doi.org/10.1016/j.solmat.2007.04.031.
[26] E. Guilmeau, D. Bérardan, C. Simon, A. Maignan, B. Raveau, D.O. Ovono, F. Delorme, Tuning the transport and thermoelectric properties of In_2O_3 bulk ceramics through doping at In-site, J. Appl. Phys. 106 (5) (2009) 053715, http://dx.doi.org/10.1063/1.3197064 ⟨⟩.
[27] R.B.H. Tahar, T. Ban, Y. Ohya, Y. Takahashi, Tin doped indium oxide thin films electrical properties, J. Appl. Phys. 83 (5) (1998) 2631–2645, http://dx.doi.org/10.1063/1.367025 ⟨⟩.
[28] A. Dolgonos, S.A. Wells, K.R. Poeppelmeier, T.O. Mason, Phase stability and optoelectronic properties of the bixbyite phase in the gallium–indium–tin–oxide system, J. Am. Ceram. Soc. 98 (2) (2015) 669–674, http://dx.doi.org/10.1111/jace.13334.
[29] O.N. Mryasov, A.J. Freeman, Electronic band structure of indium tin oxide and criteria for transparent conducting behavior, Phys. Rev. B 64 (23) (2001) 233111, http://dx.doi.org/10.1103/PhysRevB.64.233111 ⟨⟩.
[30] P. Erhart, A. Klein, R.G. Egdell, K. Albe, Band structure of indium oxide indirect versus direct band gap, Phys. Rev. B 75 (15) (2007) 153205, http://dx.doi.org/10.1103/PhysRevB.75.153205.
[31] K. Irmscher, M. Naumann, M. Pietsch, Z. Galazka, R. Uecker, T. Schulz, R. Schewski, M. Albrecht, R. Fornari, On the nature and temperature dependence of the fundamental band gap of In_2O_3, Phys. Status Solidi A 211 (1) (2014) 54–58, http://dx.doi.org/10.1002/pssa.201330184.
[32] A. Walsh, J.L.F. Da Silva, S.-H. Wei, C. Körber, A. Klein, L.F.J. Piper, A. DeMasi, K. E. Smith, G. Panaccione, P. Torelli, D.J. Payne, A. Bourlange, R.G. Egdell, Nature of the band gap of In_2O_3 revealed by first-principles calculations and X-Ray spectroscopy, Phys. Rev. Lett. 100 (16) (2008) 167402, http://dx.doi.org/10.1103/PhysRevLett.100.167402 ⟨⟩.
[33] A. Schleife, J.B. Varley, F. Fuchs, C. Rödl, F. Bechstedt, P. Rinke, A. Janotti, C. G. Van de Walle, Tin dioxide from first principles quasiparticle electronic states and optical properties, Phys. Rev. B 83 (1) (2011) 035116, http://dx.doi.org/10.1103/PhysRevB.83.035116.
[34] B.-S. Hong, S.J. Ford, T.O. Mason, Equilibrium electrical property measurements in electroceramics, Key Eng. Mater. 125–126 (1996) 163–186.
[35] F.M. Smits, Measurement of sheet resisitivities with the Four-Point Probe, Bell Syst. Technol. J. 37 (3) (1958) 711–718.
[36] D.S. McLachlan, M. Blaszkiewicz, R.E. Newnham, Electrical resistivity of composites, J. Am. Ceram. Soc. 73 (8) (1990) 2187–2203.
[39] J. Wu, W. Walukiewicz, K.M. Yu, J.W. Ager, E.E. Haller, H. Lu, W.J. Schaff, Y. Saito, Y. Nanishi, Unusual properties of the fundamental band gap of InN, Appl. Phys. Lett. 80 (21) (2002) 3967–3969, http://dx.doi.org/10.1063/1.1482786, URL ⟨⟩.
[40] A.M. White, E.W. Williams, P. Porteous, C. Hilsum, Applications of photoluminescence excitation spectroscopy to the study of indium gallium phosphide alloys, J. Phys. D. Appl. Phys. 3 (9) (1970) 1322–1328, http://dx.doi.org/10.1088/0022–3727/3/9/312.
[41] J. Weber, M.I. Alonso, Near-band-gap photoluminescence of Si-Ge alloys, Phys. Rev. B 40 (8) (1989) 5683–5693.
[42] A. Savitzky, M.J.E. Golay, Smoothing and differentiation of data by simplified least squares procedures, Anal. Chem. 36 (8) (1964) 1627–1639, http://dx.doi.org/10.1021/ac60214a047.
[43] P.D.C. King, T.D. Veal, F. Fuchs, C.Y. Wang, D.J. Payne, A. Bourlange, H. Zhang, G. R. Bell, V. Cimalla, O. Ambacher, R.G. Egdell, F. Bechstedt, C.F. McConville, Band gap, electronic structure, and surface electron accumulation of cubic and rhombohedral In_2O_3, Phys. Rev. B 79 (20) (2009) 205211, http://dx.doi.org/10.1103/PhysRevB.79.205211.

[44] A. Walsh, J.L.F. Da Silva, S.-H. Wei, Origins of band-gap renormalization in degenerately doped semiconductors, Phys. Rev. B 78 (7) (2008) 075211, http://dx.doi.org/10.1103/PhysRevB.78.075211 ⟨⟩.
[45] D.J. You, S.K. Choi, H.S. Han, J.S. Lee, C.B. Lim, Effect of the deposition geometry on the electrical properties within Tin- doped indium oxide film deposited under a given RF magnetron sputtering condition, Thin Solid Films 401 (1–2) (2001) 229–234.
[46] M.V. Hohmann, A. Wachau, A. Klein, In situ Hall effect and conductivity measurements of ITO thin films, Solid State Ion. 262 (1) (2014) 636–639, http://dx.doi.org/10.1016/j.ssi.2013.10.004 ⟨⟩.